HHS Public Access

Author manuscript

Dev Dyn. Author manuscript; available in PMC 2017 June 01.

Published in final edited form as:

Dev Dyn. 2016 June ; 245(6): 653–666. doi:10.1002/dvdy.24404.

The Vertebrate Claudin/PMP22/EMP22/MP20 family protein TMEM47 Regulates Epithelial Cell Junction Maturation and Morphogenesis

Yi Dong and **Jeffrey S. Simske**[#]

Rammelkamp Center for Education and Research, MetroHealth Medical Center, Cleveland, Ohio, USA

Abstract

Background—TMEM47 is the vertebrate orthologue of *C. elegans* VAB-9, a tetraspan adherens junction protein in the PMP22/EMP/Claudin family of proteins. VAB-9 regulates cell morphology and adhesion in *C. elegans* and TMEM47 is expressed during kidney development and regulates the activity of Fyn. The conserved functions of VAB-9 and TMEM47 are not well understood.

Results—expression of TMEM47 in *C.elegans* functionally rescues *vab-9* mutations. Unlike Claudins, expression of TMEM47 in L fibroblasts does not generate tight junction strands, instead, membrane localization requires E-cadherin expression. Temporally, TMEM47 localizes at cell junctions first with E-cadherin prior to ZO-1 co-localization and in polarized epithelia, TMEM47 co-localizes with adherens junction proteins. By immunoprecipitation, TMEM47 associates with classical adherens junction proteins, but also with tight junction proteins Par6B and aPKCλ. Over-expression of TMEM47 in MDCK cells decreases apical surface area, increases activated myosin light chain at cell-cell contacts, disrupts cell polarity and morphology, delays cell junction reassembly following calcium switch, and selectively interferes with tight junction assembly. Reduced TMEM47 expression results in opposite phenotypes.

Conclusions—TMEM47 regulates the localization of a subset of tight junction proteins, associated actomyosin structures, cell morphology, and participates in developmental transitions from adherens to tight junctions.

Introduction

Cellular junctions and their associate proteins perform a wide variety of essential functions in epithelial cells. They are critical for the establishment and maintenance of epithelial polarity, regulating the adhesive strength of tissues, regulating the passage of molecules through the paracellular space, and controlling the morphology of groups of cells, lending functional three-dimensional shape to tissues. In vertebrate epithelia there are two distinct apical cellular junction complexes, the tight and adherens junctions. The most apical junction, the tight junction, is composed of the Claudin and Occludin families of tetraspan proteins and the JAM family of single pass transmembrane proteins. Claudins are the major component of tight junction strands and function as charge-selective gaskets to mediate cell-

[#]Address correspondence to Jeff Simske, jsimske@metrohealth.org.

cell adhesion and regulate paracellular traffic (Furuse et al., 1998; Simon et al., 1999; Furuse et al., 2002). A wide variety of claudin and claudin-like proteins exist in vertebrates and invertebrates, with roles in cell adhesion and tissue morphogenesis, signal transduction, charge-selective paracellular transport, and epithelial barrier formation (Kollmar et al., 2001; Van Itallie and Anderson, 2004; Furuse and Tsukita, 2006; Gupta and Ryan, 2010; Simske and Hardin, 2011). Adherens junctions localize basal to the tight junction, but precede tight junction formation in the assembly of cell junctions following cell-cell contact (Baum and Georgiou, 2011). E-cadherin is the major transmembrane adhesive protein of the adherens junction, and mediates the initial stages of cell-cell contact and regulates the actin cytoskeleton during tissue organization and remodeling (Halbleib and Nelson, 2006; Harris and Tepass, 2010). Claudins, Occludins, and E-Cadherin signal to the actin cytoskeleton in part through interaction with cytoplasmic proteins ZO-1 and β-catenin, respectively (Ozawa et al., 1989; Itoh et al., 1999; Muller et al., 2005). Closely associated with the cellular junctions are circumferential bands of actomyosin, essential contractile components of the morphogenetic machinery that regulate epithelial shape, polarity, and migration.

Despite all that is known about the organization of the cellular junctions and their role in epithelial architecture, mysteries still remain regarding how the various junctions are assembled during development. A series of studies implicate the tight junction associated Par protein complex in regulating cell junction dynamics through interaction with the actomyosin contractile machinery, which is essential for junctional assembly and disassembly as well as cell and tissue morphology (Suzuki et al., 2002; Ivanov et al., 2004; Hildebrand, 2005; Ivanov et al., 2007; Kishikawa et al., 2008; Ishiuchi and Takeichi, 2011). For example, during cell junction re-establishment following calcium switch, knock down of Par3, aPKCλ, and Par6 results in a delay in the reformation of cell junctions, and correlative reduction in apical surface area, due to contraction of actomyosin (Chen and Macara, 2005; Ishiuchi and Takeichi, 2011). Notably, aPKCλ knock down ‘freezes’ polarizing epithelial cells in state where constricted circumferential actomyosin bands are connected to the cell membrane by actin ‘spokes’ but never incorporate into the junctions themselves(Kishikawa et al., 2008). aPKCλ activity normally counteracts actomyosin contractility, and allows incorporation of actomyosin into junctions (Kishikawa et al., 2008; Ishiuchi and Takeichi, 2011). Significantly, knock down of ZO-1/2 (MAGUK family member proteins known to associate with both adherens and tight junctions) similarly delays junction reassembly, reducing apical surface area with loss of claudin strand assembly in the tight junction (Umeda et al., 2006; Fanning et al., 2012). Collectively, these data point to a step-wise junctional assembly program, in which the Par complex and ZO-1/2 function at an intermediate step in junctional maturation, between initial adhesion mediated by the E-Cadherin/catenin complex, and the formation of the elaborate junctional strands of the tight junction. Thus, a subset of cell junction proteins regulates the transition of the circumferential actomyosin belt to a sub-membranous structure incorporated at cellular junctions. The ordered assembly of cell junctions has important consequences for normal cell structure; including establishing apical domain area and polarization.

C. elegans VAB-9 and its vertebrate orthologue TMEM47 (previously known as TM4SF10 or BCMP1) are unique claudin-like proteins in the PMP22/EMP/Claudin family, with hybrid properties of both tight and adherens junction proteins (Christophe-Hobertus et al., 2001;

Simske et al., 2003; Bruggeman et al., 2007; Azhibekov et al., 2011). In *C. elegans*, VAB-9 co-localizes with the Cadherin-Catenin complex, which resides apical and adjacent to the AJM-1/DLG-1 complex and contains the protein components of the adherens junction, including cadherin (HMR-1), α-catenin (HMP-1), β-catenin (HMP-1) and p120 (JAC-1) (Costa et al., 1998; Pettitt et al., 2003; Simske et al., 2003). The function, composition, and localization of the AJM-1/DLG-1 complex relative to the Cadherin-Catenin complex suggests this structure is analogous to the septate junction in *Drosophila*; both invertebrate structures in turn are thought to mediate tight junction-like functions, despite the inverted localization relative to the adherens junction as compared to vertebrates (Labouesse, 2006; Lynch and Hardin, 2009; Simske and Hardin, 2011; Armenti and Nance, 2012). VAB-9 functions in cell adhesion and in organizing cell morphology, since loss of *vab-9* enhances *dlg-1* or *ajm-1* loss of function cell adhesion defects, and enhances *hmp-1* embryonic enclosure and elongation phenotypes, in addition to affecting the organization of epidermal F-actin structures that correlate with the morphological body shape defects observed in *vab-9* mutant animals (Simske et al., 2003).

In vertebrate epithelial cells, TMEM47 also appears to have a developmental role in regulating the maturation of specialized cell junctions in the kidney (Bruggeman et al., 2007; Azhibekov et al., 2011).. Since the role of VAB-9 in *C. elegans* appears distinct from its vertebrate counterpart, a better understanding of TMEM47 and this class of Claudin-like proteins in vertebrate cell junction development is needed. Here the conserved function of TMEM47 and VAB-9 was tested using *C. elegans* and MDCK cells, and the consequence of TMEM47 overexpression and lack of expression on the development of cell morphology and junctional assembly was explored.

Results

Expression of TMEM47 in *C. elegans* epithelia rescues *vab-9* defects

Since VAB-9 is related, but highly divergent from murine and canine TMEM47 (VAB-9 is 27% identical to murine and canine TMEM47 at the amino acid level; murine and canine TMEM47 are 99% identical to each other), it was unclear whether these proteins would be functionally conserved. To test this directly, cDNAs for TMEM47 and TMEM47-GFP were cloned under control of the *C. elegans ajm-1* promoter, which drives expression in *C. elegans* epithelia (Simske et al., 2003), and *vab-9* mutants containing transgenic arrays composed of these constructs were tested for rescue of *vab-9* phenotypes. *vab-9* (for variably abnormal) animals hatch with morphological defects, but mature to fertile adults. All animals have tail defects with variable body shape defects (are dumpy), and occasionally are egg-laying defective as adults. Animals were scored as ‘rescued’ for *vab-9* defects if they showed none of the *vab-9* phenotypes, that is, they were indistinguishable from wild-type animals at all stages. Both TMEM47 and TMEM47-GFP proteins strongly rescued the *vab-9* defects resulting from the null deletion allele *ju6,* and correctly localized to cell junctions, similar to the localization pattern of the native *C. elegans* VAB-9 protein (Fig. 1A,B, and D). This experiment indicates core functions are conserved between VAB-9 and TMEM47 in epithelial cells, and that the GFP tagged TMEM47 protein is fully functional.

TMEM47 has predicted intracellular amino (N)- and carboxy (C)-termini and four transmembrane domains generating one intracellular and two extracellular loops (Fig.1C). Interestingly, TMEM47 expression rescues *vab-9* phenotypes, even though TMEM47 terminates with a di-tyrosine, whereas VAB-9 extends 15 residues further. To determine whether distinct regions of TMEM47 mediate specific functions, TMEM47-GFP and mutated forms of TMEM47-GFP were introduced into *vab-9* mutants and TMEM47-GFP localization and *vab-9* phenotypic rescue were scored (Fig.1D-V). TMEM47(ΔN)-GFP localized in a largely normal pattern at the apical junctional complex, with localization to the lateral cell membranes in epidermis and pharynx, and rescued all *vab-9* defects, including tail, body shape and egg-laying defects in adults (Fig.1G-J). *vab-9* mutants display disruptions in the organization of circumferential F-actin filaments that are required for smooth elongation of the embryo into the characteristic worm shape. Expression of full-length TMEM47, the N-terminal deletion, and the Y180/181A "YA" variant, but not the C-terminal deletion, restore the normal organization of filaments in the epidermis of *vab-9* mutants (Fig.1 O-R). Deletion of the entire cytoplasmic C-terminus results in undetectable TMEM47(ΔC)-GFP in the embryonic epidermis so that localization at the adherens junction complex in this tissue could not be scored. However, in the pharynx and the hermaphrodite vulva (not shown), diffuse cytoplasmic expression of TMEM47(ΔC)-GFP suggests this truncated protein fails to localize to the cell membrane (Fig.1N). This is similar to the mislocalization of VAB-9 observed in *hmr-1* mutant embryos, suggesting that the C-terminal cytoplasmic domain mediates cadherin-dependent localization (Simske et al., 2003). TMEM47(ΔC)-GFP failed to rescue *vab-9* phenotypes. A doubly mutated TMEM47-GFP ("TMEM47YA-GFP") protein that substituted the two C-terminal tyrosines with alanines was used to test whether these tyrosines participated in the trafficking of TMEM47 to the cell membrane or focusing localization at the adherens junction complex. This protein mislocalized to the basolateral membrane (Fig. 1F,T), a typical result of polarity defects, suggesting that the C-terminus of TMEM47 is responding to polarity cues. Like TMEM47(ΔN)-GFP, overexpression of TMEM47(YA)-GFP rescued *vab-9* mutant defects, suggesting that sufficient TMEM47 is still present at cell junctions and remains functional, or that mislocalized TMEM47 is capable of performing normal VAB-9 functions.

TMEM47 associates with the adherens junction in MDCK cells

VAB-9 specifically localizes with adherens junction proteins in *C. elegans* epidermal cells (Simske et al., 2003), suggesting that TMEM47 may co-localize with the same cell junction in vertebrate epithelia. To determine whether VAB- 9 and TMEM47 localization patterns are similar, the expression patterns of endogenous TMEM47 and exogenously expressed TMEM47-GFP and VAB-9-GFP were compared in MDCK cells (Fig. 2). Each protein showed similar prominent apical junctional localization, with the exception that overexpressed, tagged TMEM47 and VAB-9 showed stronger staining in the perinuclear region and in puncta localizing from the perinuclear region to the cell membrane. In some preparations, VAB-9 and TMEM47 antibodies also recognize a nuclear epitope. In fully polarized MDCK cells stably expressing TMEM47-GFP and co-stained with junctional antibodies, TMEM47-GFP co-localized along the lateral membrane with E-cadherin and β-catenin (Fig. 2, columns C and E), but only some co-localization of TMEM47-GFP and ZO-1 was apparent at the most basal extreme of ZO-1 localization (Fig. 2D), which may

account for the co-localization observed when the top focal planes were co-projected as in Figure 2B. Co-localization of TMEM47-GFP with F-actin at cell contacts was also observed (Fig. 2, row F). Finally, *C. elegans* VAB-9 tagged with GFP shows similar localization to TMEM47-GFP when expressed in MDCK cells (Fig. 2G).

TMEM47 associates with nascent junctions in MDCK cells

MDCK cells stably expressing TMEM47-GFP were used to examine the dynamics of TMEM47 localization during the development of cell contacts (Fig 3). Prior to cell contact, TMEM47-GFP was concentrated in the perinuclear region, but was also found in intracellular vesicles of various sizes throughout the cytoplasm (Fig 3A). In co-staining experiments, TMEM47-GFP expression overlapped most significantly with β-catenin in intercellular structures and with E-Cadherin at the membrane of non-contacting MDCK cells. Overlapping localization with occludin was much less significant. Upon initiation of cell contact, TMEM47 was first visible co-localized with E-Cadherin at nascent cell-cell contacts, organized into short filaments orthogonal to the plane of cell-cell contact (Fig.3B). In these nascent contacts, a subset of TMEM47-GFP containing contacts lacked ZO-1, but all ZO-1 contacts contained TMEM47-GFP, suggesting that TMEM47-GFP localizes at nascent contacts with E-Cadherin prior to ZO-1 localization. Upon formation of stable cell contacts prior to the development of pronounced apical-basal polarity, TMEM47-GFP localization was almost completely co-incident with E-cadherin and ZO-1 along regions of cell-cell contact (Fig. 3C). Since TMEM47 and β-catenin appeared to be closely associated, TMEM47-tagRFP and β-catenin-Emerald were co-expressed, showing that these two proteins often move in concert during junctional reorganization in MDCK cell sheets (Fig. 3D,E and supplement).

Since cadherin is required for VAB-9 junctional localization in *C. elegans*, the ability of TMEM47 to localize at cell contacts was tested directly in murine L cells, which do not express E-cadherin (Chen and Obrink, 1991). When expressed alone in L cells, TMEM47-GFP remained in the perinuclear region (Fig. 3F), however, when co-expressed with E-Cadherin, TMEM47-GFP co-localized at cell contacts with E-cadherin (Fig. 3G). Together with earlier results (Fig.1) these results suggest that the C-terminal cytoplasmic domain is required for cell membrane localization, localization to the adherens junction complex is dependent on E-Cadherin, and the C-terminal tyrosines may be specifically involved in focusing TMEM47-GFP at the adherens junction complex.

Since co-localization experiments in MDCK cells suggested that TMEM47 and ZO-1 localize independently, we tested the localization of ZO-1 orthologue ZOO-1 in *vab-9* animals. Previously, ZOO-1 was reported to require VAB-9 for junctional localization (Lockwood et al., 2008). Surprisingly, we found that ZOO-1 and ZOO-1-GFP localized normally to cell junctions in our experiments (Fig. 3H-L). ZOO-1-GFP localized to seam cell junctions prior to and after the expression of the *vab-9* body and tail shape defects (Fig. 3, columns I and J). These results are consistent with the vertebrate findings, supporting cross-species conservation of basic functions.

TMEM47 Overexpression affects tight junction protein localization

While immunostaining MDCK cells transiently transfected with TMEM47-GFP, we discovered that TMEM47-GFP overexpression blocked junctional localization of several tight junction proteins, including occludin and claudin (Fig. 4B and C). In the case of Claudin 1, increased cytoplasmic localization of claudin 1 coincided with reduced junctional localization (Fig. 4E). In contrast, the localization of ZO-1, E-cadherin, and β-catenin appeared to be unaffected (Fig. 4H, Fig. 2, Fig. 3).

TMEM47 associates with catenins, aPKCλ and Par6B and regulates aPKCλ and PAR6 junctional localization

TMEM47 co-localization with adherens junction proteins and tight junction proteins during junctional maturation suggested that TMEM47 might interact directly with adherens and tight junction proteins. To begin to address possible protein-protein interactions, TMEM47 was tested for the ability to co-immunoprecipitate with various junctional proteins. Immunoprecipitations were carried out with antibodies against endogenous TMEM47 and antibodies that precipitate Myc or GFP-tagged versions of TMEM47 either transiently or stably expressed in MDCK cells. Immunoprecipitates were tested for the presence of various adherens and tight junction proteins. E-Cadherin and tight junction proteins occludin, claudin-1, ZO-1, and PAR-3 did not co-immunoprecipitate with TMEM47. Only α-catenin, β-catenin, aPKCλ–myc and Par6B co-immunoprecipitated with TMEM47 tagged with GFP, but the precipitating fraction was very small (less than 5%), suggesting that association of these proteins with TMEM47 is weak, transient, or indirect.

Since TMEM47 appears to associate with the PAR protein complex, the effect of TMEM47-GFP over-expression on Par6B and aPKCλ localization was examined. Like occludin and claudin1, junctional localization of Par6B and aPKCλ was disrupted in TMEM47-GFP cells (Fig. 5D-G). Like claudin1, some aPKCλ localized to the cytosol, in a pattern similar to over-expressed TMEM47-GFP. The effect of TMEM47 reduction on Par6B was tested by inactivating *Tmem47* using gene silencing by RNA interference (RNAi) with plasmids expressing short hairpin (sh)RNAs (see Methods). Par6B localization was affected in *Tmem47* shRNA cells, except that in contrast to TMEM47-GFP cells, Par6B appeared more concentrated in the nucleus (Fig.5H). In *Tmem47* shRNA cells, β-catenin localization appeared essentially normal (Fig. 5I) and both Par6B and β-catenin localized normally in control transfections.

TMEM47 expression levels regulate cell junction reformation following calcium switch and apical surface area

The role of TMEM47 in the regulation of cell junctions and cell morphology was further examined in cells overexpressing TMEM47-GFP and in *Tmem47* shRNA cells. First, cell junction reformation following calcium switch was scored (Fig. 6). Cells stably expressing TMEM47-GFP were plated to confluence, grown for 20 hours in low calcium medium, and assayed for junction reformation following return to normal calcium levels. Cells expressing TMEM47-GFP showed a strong delay in junction reformation, extending for over three hours after re-addition of calcium, based on E-cadherin and ZO-1 localization (Fig. 6 C,D, G, and H). Following junctional reformation, TMEM47-GFP overexpressing cells display

non-uniform concentrations of cell junction proteins E-Cadherin and ZO-1 as well as disorganized cell junctions (Fig. 6D,H). Since overexpression of TMEM47-GFP resulted in morphological defects and delay in junction formation following calcium switch, it seemed likely that knock down of TMEM47 would result in opposite phenotypes. To test this, TMEM47 was inactivated in MDCK cells using *TMEM47* shRNA. Expression of *TMEM47* shRNA strongly reduced endogenous TMEM47 in Western blots (see Fig. 7T). MDCK cells transiently transfected with two different *Tmem47* shRNA constructs or a control shRNA with three mutations were subjected to calcium switch and cell junction reformation was similarly monitored by ZO-1 staining. Following calcium switch, control cells displayed slower junctional reformation, higher cytoplasmic ZO-1 staining, and more small, junctional rings compared to *Tmem47* shRNA cells (Fig. 6I-K). Two different shRNAs were tested and compared to the control; the average of three separate experiments were quantified (Fig.6K).

To determine the nature of the morphological defects caused by TMEM47-GFP over-expression, cell mixing experiments between MDCK cells and MDCK cells stably expressing TMEM47-GFP were carried out to compare normal and overexpressing cells side-by-side. In mixed cell populations, TMEM47-GFP over-expressing cells showed decreased apical surface areas relative to normal cells (300±22mm^2 versus 639±38mm^2 for controls; N=36 and 38 respectively, P<0.0001) (Fig. 7A-D). Decreased area of TMEM47-GFP cells was also observed following phalloidin staining for F-actin in homogeneous populations of cells (Fig.7E-H). Interestingly, the number of ventral stress fibers/cell in control MDCK and TMEM47-GFP cells are not significantly different (2.54±.06 and 2.47±0.18 stress fibers/cell, respectively, p=0.51, n=67 cells in 3 experiments) but due to the decreased area of TMEM47-GFP cells, the density of fibers in TMEM47-GFP cells is approximately two-fold higher (8.3×10E-4 vs. 3.9×10E-4 Fibers/μm^2). In the converse experiment, *Tmem47* shRNA cells showed increased apical surface area (1438±522mm^2 versus 708±166mm^2 for controls; N=28 and 32 respectively' P<0.0001) (Fig. I-L). Interestingly, actin levels at cell contacts also appeared to be reduced (Fig. 7J).

Based on staining with cell junction proteins E-cadherin and ZO-1, TMEM47-GFP cells also appear to have altered morphology, in which cell junction proteins and cell junctions are unevenly distributed in the cell sheet layer (Fig. 6D, 6H). The mechanisms of cell surface area regulation have recently been described for cell junction proteins like ZO-1/2, aPKCλ and Par6, and in several cases, the altered surface area is a consequence of altered localization and/or activation of the actomyosin contractile machinery downstream of cell junction proteins (Ishiuchi and Takeichi, 2011; Fanning et al., 2012). To test whether TMEM47 is influencing the same process, TMEM47-GFP expressing cells were scored for localization and levels of the active, phosphorylated (serine 19) form of myosin light chain kinase (p-MLC). There is a correlation between TMEM47 expression and morphological phenotypes: the highest expressing TMEM47-GFP cells have reduced apical surface areas, and increased concentrations of F-actin and active myosin light chain (p-MLC) along regions of cell-cell contact (Fig. 7M-S). We tested whether TMEM47 overexpression results in an overall increase in p-MLC levels and found that there is no significant difference from controls (in arbitrary units 10001±5569 versus 13278±6129 for control MDCK cells and TMEM47-GFP cells, respectively, N=3, p=0.4588). (Fig.7P). In the converse experiment, p-MLC levels appear reduced in TMEM47 shRNA MDCK cells (in arbitrary units 6928±3512

versus 661±46 for control and shRNA cells, respectively, N=3, p= 0.0372) (Fig. 7T,U)., Together these results suggest that TMEM47 positively regulates actomyosin activity.

Discussion

The findings presented here demonstrate that TMEM47 is an evolutionarily conserved adherens junction protein involved in regulating cell junction organization in MDCK cells. Generally, these results suggest a model whereby TMEM47 functions as a governor during the transition from adherens to tight junctions, supported by several findings presented in this study. First, based on localization, TMEM47 is positioned developmentally between adherens junction and tight junction assembly. TMEM47 displays co-localization with adherens junction proteins both in the cytoplasm of non-contacting cells before the assembly of nascent cell junctions to the formation of the polarized columnar epithelial cell phenotype. In contrast, TMEM47 does not show the same localization with tight junction proteins either before cell contact or in mature junctions. Significantly, TMEM47 localizes at cell junctions independently from tight junction proteins, placing TMEM47 localization between adherens junction and tight junction during junctional assembly. The requirement for adherens junction localization prior to TMEM47 placement is further supported by the finding that E-cadherin expression is required for TMEM47 localization to cell contacts in L fibroblasts. Second, *Tmem47* shRNA and over-expression have opposite affects on the nature of cell junction assembly and tissue morphogenesis. Specifically, TMEM47 knock-down results in an increase in apical surface area, an increase in the rate of cell junction reassembly following calcium switch, and a decrease in p-MLC levels. TMEM47 over-expression results in a decrease in apical surface area, delay in junction reformation, and an increase in phosphorylated myosin light chain at regions of cell contact. Third, TMEM47 over-expression blocks or delays the localization of some tight junction proteins (Claudin1, Occludin, Par6B, and aPKCλ), but does not affect ZO-1 or adherens junction protein localization. These results, together with the observation that a fraction of TMEM47 co-immunoprecipitated with adherens proteins and with the tight junction proteins Par6 and aPKCλ, suggest that TMEM47 may transiently interact with junctional proteins specifically to regulate the process of junctional maturation, following adherens junction assembly and prior to complete tight junction formation.

The sequential development of distinct cell junctions is an established property of epithelia. Initial cell-cell contact in epithelial cells occurs via actin-rich filopodia from adjacent cells. Spot-like junctional “primordia” composed of adherens junction proteins localize with actin-polymerization machinery at nascent contacts between vertebrate epithelial cells (keratinocytes, fibroblasts) and enclosing ventral epithelia in *C. elegans* (Yonemura et al., 1995; Adams et al., 1998; Raich et al., 1999; Vasioukhin et al., 2000; Vaezi et al., 2002; Zhang et al., 2005). Expansion of adherens junctions depends on actin polymerization, but a series of studies indicate that spot adhesions mature into circumferential cell adhesions also under the control of the ZO-1 and the Par protein complex, which in part function via regulation of actomyosin contraction, and that development of elaborated tight junctions depends on the proper execution of these early steps. (Suzuki et al., 2002; Ivanov et al., 2004; Ivanov et al., 2007; Kishikawa et al., 2008; Van Itallie et al., 2009; Ishiuchi and Takeichi, 2011; Fanning et al., 2012). One unique feature of *Tmem47* knock down was the

more rapid re-assembly of cellular junctions upon re-addition of calcium to depleted cells. More rapid assembly of tight junction proteins was also observed in T84 cells upon treatment with Jasplakinolide, which stimulates F-actin polymerization, suggesting that TMEM47 may influence F-actin polymerization required for normal tight junctional localization dynamics (Ivanov et al., 2005).

TMEM47 incorporation into nascent cell-cell contacts is coincident with E-cadherin and often independent of ZO-1, suggesting that TMEM47 function is at least partially independent of ZO-1. Similar to TMEM47-GFP overexpression, in ZO-1/2 knock down cells, the localization of only a subset of tight junction proteins (CLDN1 and occludin) is affected (Fanning et al., 2012). Since TMEM47 overexpression altered the localization of Claudin1 (CLDN1) and Occludin without affecting ZO-1 or adherens junction protein localization, TMEM47 likely acts in parallel and possibly downstream of ZO-1, and thus participates in only some ZO-1/2 functions. TMEM47 orthologue VAB-9 appears to function in a similar position in the junctional development hierarchy in *C. elegans*, where the cadherin HMR-1 is required for VAB-9 localization but VAB-9 in turn is not required for ZO-1 orthologue ZOO-1 recruitment to cell junctions. Our findings of ZOO-1 localization in *vab-9* contrast with those of a previous study(Lockwood et al., 2008). In that study, ZOO-1-GFP localization in *vab-9* was not tested, likely because the integrated ZOO-1-GFP reporter is tightly linked to *vab-9*. We found that ZOO-1 epidermal detection in the embryonic seam cells was highly sensitive to fixation and staining conditions, possibly explaining differences in findings (Simske et al., 2003; Lockwood et al., 2008). While the specific junctional proteins affected by VAB-9 and TMEM47 may differ between systems, these findings suggest a conserved localization hierarchy in which TMEM47/VAB-9 is downstream of E-Cadherin and upstream and parallel to tight junction proteins during cell junction development. Significantly, since cell junctions still form in the absence of TMEM47, it seems most likely that TMEM47 is acting as a governor of tight junction assembly rate and morphology, rather than being strictly required for junctional formation.

Claudin proteins expressed in L fibroblasts generally organize into tight junction strands whereas TMEM47 that localized with E-cadherin junctions in L cells did not appear to form strands, suggesting that TMEM47 does not generally behave like a classic claudin. Binding of the C-terminal PDZ ligand to the PDZ domain in MAGUK proteins like ZO-1/2 is thought to be required for polymerization of strands. However, TMEM47 lacks a typical PDZ ligand, and localizes to cell contact independently of ZO-1, thus it is not surprising that an alternate mechanism for incorporation into cell contacts may be used and that assembly and function at cell contacts may be distinct from classic claudins (Itoh et al., 1999; Umeda et al., 2006; Simske, 2013). It is of interest to note that some claudins family members such as Claudin 7, localize basolaterally in kidney epithelia and have function independently of cell junctions(Gonzalez-Mariscal et al., 2006; Lu et al., 2015). TMEM47 shows similar basolateral localization in the mouse kidney, possibly in distal convoluted tubules or the thick ascending limb(Bruggeman et al., 2007). We showed that mutated TMEM47 with an N-terminal deletion or mutated C-terminal di-tyrosines displayed more basolateral localization. While remaining junctional localization of TMEM47 variants may be sufficient for rescue of *vab-9* phenotypes, it is also possible that basolaterally mislocalized TMEM47 variants are still able to perform sufficient VAB-9 functions for rescue.

At least two observations suggest an interaction between TMEM47 and the actomyosin machinery. First, TMEM47 expression levels influence F-actin organization; overexpression reduced stress fiber levels and increased F-actin concentration at regions of apical cell contact, while knock down appeared to reduce junctional F-actin levels. Second, TMEM47 overexpression results in cell morphological changes that are reminiscent of those observed upon overexpression of the actin binding protein Shroom (Hildebrand, 2005). Shroom expression regulates cell morphology directly through apical constriction of actomyosin, and may have a general role in such processes, particularly during neural tube closure (Hildebrand and Soriano, 1999; Haigo et al., 2003; Hildebrand, 2005).

It has been well-established that apical surface area is regulated by actomyosin contractility. Reduction in apical surface area correlates with increased levels of phosphorylated junctional myosin regulatory light chain, changes in sub-cellular actin accumulation, and is observed in ZO-1/2, Par3, Par6, and Cdc42 knock down epithelial cells (Georgiou et al., 2008; Ishiuchi and Takeichi, 2011; Fanning et al., 2012). Here, over-expression of TMEM47 similarly correlated with increased levels of phosphorylated junctional myosin regulatory light chain at cell contacts and reduced apical surface area, while RNAi inactivation results in expanded surface area and reduced p-MLC levels, indicating that TMEM47 may be involved in similar pathways that regulate actomyosin contractility. Absolute p-MLC levels are only altered upon TMEM47 knock-down, which is consistent with mechanisms whereby TMEM47 regulates activated myosin light chain localization, stabilization, or both.

TMEM47 interactions suggest a role in a subset of Par protein complex functions. TMEM47 co-immunoprecipitated with aPKCλ and Par6B, but not Par3 or other tight junction proteins, indicating a more specific role with this subset of junctional proteins. In Eph4 mammary cells, aPKCλ and Par6B are recruited independently of Par3 to cell junctions by Willin and regulate contractility via phosphorylation and localization of ROCK (Rho-associated kinases) (Ishiuchi and Takeichi, 2011). Loss of aPKCλ and Par6 activity results in hyper-contraction of actomyosin, similar to overexpression of TMEM47, pointing to a role forTMEM47 in the negatively regulation of Par6B and aPKCλ activity. Localization of Par6B and aPKCλ are both sensitive to TMEM47 levels, since overexpression of TMEM47-GFP causes mislocalization of both proteins, and reduction in TMEM47 via shRNA appears to reduce junctional Par6B localization. Mislocalization of Par6B in TMEM47-GFP over-expressing cells correlates with increased apical actin and P-MLC levels, and reduced apical surface area, supporting a model whereby TMEM47 positively regulates actomyosin-driven apical morphogenesis via negative regulation of Par6B and aPKCλ. More broadly, TMEM47 may regulate apical identity through Par6B and aPKCλ, as in *Xenopus* epidermis where Par6B represses apical and promotes basal epithelial characteristics (Wang et al., 2013). Alternatively, TMEM47 may have a more limited role, as it has been shown that unlike TMEM47, Par6B overexpression affects the localization of both peripheral and structural junctional components, including ZO-1, so that TMEM47 may regulate only a subset of Par6 functions (Gao et al., 2002). (Verma et al., 2003; Li et al., 2004; Jones et al., 2006; Azhibekov et al., 2011)

Experimental Procedures

C. elegans immunocytohistochemistry, strains, and transfection

Embryos were fixed and stained using a freeze-fracture methanol technique as described (Simske et al., 2003). Goat anti-rabbit or mouse rhodamine red X or Cy2 secondary antibodies (Jackson Immunoresearch,West Grove, PA) were used for antibody detection. Phalloidin staining of F-actin in embryos was performed as described (Cox-Paulson et al., 2014). For rescue experiments, *C. elegans* hermaphrodites were transfected with murine TMEM47 expression plasmids (described below) for extrachromosomal expression using standard methods as previously described(Simske et al., 2003). Target plasmids (10 ng/μl), and co-injection markers pRF4 (confers a dominant rolling phenotype) (100 ng/μl,) or pDPMM0168 (rescues *unc-119*) (80 ng/μl,) were injected together into wild-type or *unc-119(ed3)* animals, and roller or non-unc lines were recovered. We discovered that the *zoo-1::gfp* integrated array *jcIs22* is located nearby *vab-9* on LGII (Lockwood et al., 2008). To generate *vab-9, jcIs22[pRF4,zoo-1::gfp]* animals, rare Vab Rol animals (1 in 300 Vabs) were recovered from *vab-9/jcIs22[pRF4,zoo-1::gfp]* heterozygotes, and v*ab-9, jcIs22[pRF4,zoo-1::gfp]* homozygotes were selected.

Cultured Cells and immunostaining

Except where noted, L fibroblasts and MDCK cells were grown on coverslips or treated plastic culture dishes. For polarized cell growth, cells were plated to confluence (2.5×10^6 cell/6 well) on 0.45μm collagen coated polycarbonate filters (Costar, Corning, Tewksbury, MA). For immunostaining, cells were washed with PBS and fixed for 10-20 minutes with 1% formaldehyde in PBS, followed by a 3min permeabilization wash in 0.1% triton X-100 and equilibrated in 1% BSA, 0.1% tween 20, 0.01% sodium azide in 1XPBS for 1 day. Primary antibody incubation was carried out in 10-20μl volumes under coverslips at 4°C for 1 day, washed three times in blocking buffer, and secondary antibody incubations were carried out for 2 hours under coverslip with the respective species-absorbed fluorescent goat antibodies (Jackson Immunoresearch). DAPI or TOPRO3 were added in the final wash where indicated; coverslips were mounted with DABCO and sealed with nail polish.

Antibodies

TMEM47 polyclonal antibodies raised in rabbits against the cytoplasmic C-terminal peptide (CLNPKNYEDYY) were generated by Biosource (Life Technologies, Grand Island, NY). E-Cadherin, ZO-1, Occludin, and Claudin 1 antibodies were purchased from Zymed (Life Technologies), PKCλ from Transduction Labs (BD Biosciences, San Jose, CA), Par6A from Santa Cruz Bitoech (sc-14405, Santa Cruz, CA), and Par6B was from Sigma (#B8062) or a gift from James Nelson (Stanford University). F-actin was identified by incubation with TRITC-labeled phalloidin (Sigma Aldrich, St. Louis, MO) as previously described (Azhibekov et al., 2011) . Rabbit anti-ZOO-1 antibody was a gift from Jeff Hardin (University of Wisconsin) and used at 1:100 dilution.

Imaging

Image stacks were captured using Metaview software on a Nikon E600 inverted scope and deconvolved using Autoquant version 8.0 deblur software. Equivalent images were also captured on a Leica DMRE confocal microscope. Some images and video captures were processed using ImageJ software with iterative deconvolving 3D plugin. Western blot bands were quantified using ImageJ. Images were imported into Photoshop and Illustrator for creation of figures. Some figure panels have gamma adjustments, noted in figure legends. Live imaging was carried out in FCS3 chamber (Bioptics, Butler, PA). MDCK cells stably expressing β-catenin-Emerald were transfected with TMEM47-tagRFP and sequential images from red and green channels from co-expressing cells were captured at 20 second intervals for 20 minutes. Movies were edited in ImageJ and Quicktime.

Plasmids

Green fluorescent protein (GFP) and-myc-tagged plasmids were constructed by cloning the murine TMEM47 (*tmem47*) or aPKCλ (*prkci*) cDNAs into pEGFPN2 or pcDNAmyc using standard methods. The VAB-9::GFP expression plasmid has been previously described (Bruggeman et al., 2007; Azhibekov et al., 2011). For expression of TMEM47 in *C. elegans* epithelia, murine TMEM47 and TMEM47-GFP were cloned into a plasmid containing the *C. elegans ajm-1* promoter and 3′ untranslated region(Koppen et al., 2001; Simske et al., 2003), TMEM47 plasmids with N-terminal (deletion of amino acids 1-20, MASAGSGMEEVRVSVLTPLK, “ΔN”) and C-terminal (deletion of amino acids 173-181, YCLNPKNYEDYY, “ΔC”) were produced using PCR amplification, and the plasmid with carboxy terminal tyrosine residues at 180 and 181 changed to alanines (“YA”) was made using using site directed mutagenesis (Life Technologies). Plasmids expressing shRNAs were made by cloning complimentary oligonucleotide pairs into pG-SUPER (Kojima et al., 2004). The following sequences were used for canine *Tmem47*: GGCGCTTCTACAGACCTGT (shRNA1), CCCTAAGAACTACGAAGAC (shRNA2); and a control which contains three mutations in the canine *Tmem47* sequence (bolded) GGC**A**CTTC**G**ACAGAC**A**TGT that lacked shRNA activity. TMEM47 shRNA transfected cells were identified by GFP fluorescence using pG-SUPER plasmids, since GFP is expressed from the same plasmid as the shRNA (Kojima et al., 2004). Using Lipofectamine 2000 (Life Technologies) Transfection efficiencies were typically greater than 60%. Sequences are based on canine *Tmem47*, accession number NP_001003045.1. mEmerald-Beta-Catenin-20 was a gift from Michael Davidson (Addgene plasmid # 54017).

Immunoprecipitation and Western Blotting

Cell from 150mm culture plates were washed three times with ice cold PBS, incubated on ice for 20 min, in adjusted CSK buffer (100mM NaCl, 300mM sucrose, 3mM $MgCl_2$, 10mM PIPES pH6.8 with protease inhibitor cocktail (Roche, Indianapolis) (Hinck et al., 1994) (These conditions were used for tight junction proteins, catenins, Par6 and aPKCλ immunoprecipitations) or in a buffer of 50mM Tris pH7.4, 150mM NaCl, 10% Glycerol, 1% Triton X-100, 1.5mM $MgCl_2$, 1mM EGTA, 10mM NaF, 10mM $Na_4P_2O_7$, 1mM Na_3VO_5, 1 mM phenylmethylsulfonyl fluoride (these conditions were used for non-muscle myosin proteins, tight junction proteins, catenins and E-cadherin immunoprecipitations)(Hurd et al.,

2003), followed by scrape recovery, vortexed for 5-10sec and spun at 10,000rpm (6121*xg*) in a microfuge. 100μl of soluble fraction lysate were saved for lysate controls and 900μl was incubated with protein G sepharose and rabbit polyclonal mouse, or goat polyclonal IgG for 2 hours at 4°C to precipitate non-specific interacting proteins. Supernatant was then split and incubated with primary antibody or control polyclonal antibody and precipitated with protein G sepharose, washed 5 times with HEPES/Triton buffer and boiled for 10 min in gel loading buffer. Denaturing polyacrylamide gels were run and transferred to PDVF membranes for Western blotting. Membranes were blocked with 5% non-fat milk, 2% BSA, in (10mM Tris pH 7.4, 140mM NaCl, 0.1% Tween 20), and primary antibody was added at 1:500 dilution for rabbit polyclonal anti-TMEM47 antibodies, and 1:2000 for mouse monoclonal antibodies against Occludin, Claudin, ZO-1, E-Cadherin, β-Catenin, and α-Catenin. Detection was via chemiluminescence (ECL Plus, GE Life Sciences, Pittsburgh, PA) according to manufacturer's instructions.

Transfection

Cells were plated at the recommended density and transfected with Lipofectamine 2000 (Life Technologies) according to manufacturer's instructions to greater than 60% efficiency. Stably expressing lines were selected at limiting dilution for neomycin resistance with geneticin G418 and recovered with clone rings.

Calcium Switch

MDCK cells, stably transformed lines, or transiently transfected lines were grown to confluence in standard growth media (with G418 for selection for stably transformed lines) in 6 well dishes with coverslips. Medium was replaced with low calcium medium (2-4μM Ca^{2+}) for 20 hours and then replaced with high calcium medium (1.8mM Ca^{2+}) and incubated for indicated times prior to fixation and staining or extraction. Cell junctions with greater than 75% circumferential ZO-1 were scored as ‘re-established.’

Statistics

All statistical calculations, including standard deviations, Student t-tests and two-tailed ANOVA tests were carried out by running StatPlus®:mac software (AnalystSoft Inc., Alexandria, VA) within Microsoft Excel.

Supplementary Material

Refer to Web version on PubMed Central for supplementary material.

Acknowledgments

This work was supported by Public Health Service grant DK-095832 from the National Institute of Diabetes and Digestive and Kidney Diseases and a grant from the MetroHealth Foundation. Some strains were provided by the CGC, which is funded by NIH Office of Research Infrastructure Programs (P40 OD010440). We thank Leslie Bruggeman for critical review and editing of the manuscript, Bingcheng Wang for supplies and laboratory space, Hui Maio for expert technical training with tissue culture, Linda Lund for technical assistance, and James Nelson for antibodies and E-Cadherin reagents. We thank Jeff Hardin and Allison Lynch for ZOO-1 reagents and technical assistance with ZOO-1 staining and analysis. We thank anonymous reviewers for their input, which improved the paper. This paper is dedicated to the memory of Hui Miao, who was an exceptional scientist and friend.

Grant Sponsor: National Institute of Diabetes and Digestive and Kidney Diseases

Grant Number: DK-095832

References

Adams CL, Chen YT, Smith SJ, Nelson WJ. Mechanisms of epithelial cell-cell adhesion and cell compaction revealed by high-resolution tracking of E-cadherin-green fluorescent protein. J Cell Biol. 1998; 142:1105–1119. [PubMed: 9722621]

Armenti ST, Nance J. Adherens junctions in C. elegans embryonic morphogenesis. Subcell Biochem. 2012; 60:279–299. [PubMed: 22674076]

Azhibekov TA, Wu Z, Padiyar A, Bruggeman LA, Simske JS. TM4SF10 and ADAP interaction in podocytes: Role in Fyn activity and Nephrin phosphorylation. Am J Physiol Cell Physiol. 2011

Baum B, Georgiou M. Dynamics of adherens junctions in epithelial establishment, maintenance, and remodeling. J Cell Biol. 2011; 192:907–917. [PubMed: 21422226]

Bruggeman LA, Martinka S, Simske JS. Expression of TM4SF10, a Claudin/EMP/PMP22 family cell junction protein, during mouse kidney development and podocyte differentiation. Dev Dyn. 2007; 236:596–605. [PubMed: 17195181]

Chen WC, Obrink B. Cell-cell contacts mediated by E-cadherin (uvomorulin) restrict invasive behavior of L-cells. J Cell Biol. 1991; 114:319–327. [PubMed: 1649199]

Chen X, Macara IG. Par-3 controls tight junction assembly through the Rac exchange factor Tiam1. Nat Cell Biol. 2005; 7:262–269. [PubMed: 15723052]

Christophe-Hobertus C, Szpirer C, Guyon R, Christophe D. Identification of the gene encoding Brain Cell Membrane Protein 1 (BCMP1), a putative four-transmembrane protein distantly related to the Peripheral Myelin Protein 22 / Epithelial Membrane Proteins and the Claudins. BMC Genomics. 2001; 2:3. [PubMed: 11472633]

Costa M, Raich W, Agbunag C, Leung B, Hardin J, Priess JR. A putative catenin-cadherin system mediates morphogenesis of the Caenorhabditis elegans embryo. J Cell Biol. 1998; 141:297–308. [PubMed: 9531567]

Cox-Paulson E, Cannataro V, Gallagher T, Hoffman C, Mantione G, McIntosh M, Silva M, Vissichelli N, Walker R, Simske J, Ono S, Hoops H. The minus-end actin capping protein, UNC-94/tropomodulin, regulates development of the Caenorhabditis elegans intestine. Dev Dyn. 2014; 243:753–764. [PubMed: 24677443]

Fanning AS, Van Itallie CM, Anderson JM. Zonula occludens-1 and -2 regulate apical cell structure and the zonula adherens cytoskeleton in polarized epithelia. Mol Biol Cell. 2012; 23:577–590. [PubMed: 22190737]

Furuse M, Hata M, Furuse K, Yoshida Y, Haratake A, Sugitani Y, Noda T, Kubo A, Tsukita S. Claudin-based tight junctions are crucial for the mammalian epidermal barrier: a lesson from claudin-1-deficient mice. J Cell Biol. 2002; 156:1099–1111. [PubMed: 11889141]

Furuse M, Sasaki H, Fujimoto K, Tsukita S. A single gene product, claudin-1 or -2, reconstitutes tight junction strands and recruits occludin in fibroblasts. J Cell Biol. 1998; 143:391–401. [PubMed: 9786950]

Furuse M, Tsukita S. Claudins in occluding junctions of humans and flies. Trends Cell Biol. 2006; 16:181–188. [PubMed: 16537104]

Gao L, Joberty G, Macara IG. Assembly of Epithelial Tight Junctions Is Negatively Regulated by Par6. Curr Biol. 2002; 12:221–225. [PubMed: 11839275]

Georgiou M, Marinari E, Burden J, Baum B. Cdc42, Par6, and aPKC regulate Arp2/3-mediated endocytosis to control local adherens junction stability. Curr Biol. 2008; 18:1631–1638. [PubMed: 18976918]

Gonzalez-Mariscal L, Namorado Mdel C, Martin D, Sierra G, Reyes JL. The tight junction proteins claudin-7 and -8 display a different subcellular localization at Henle's loops and collecting ducts of rabbit kidney. Nephrol Dial Transplant. 2006; 21:2391–2398. [PubMed: 16766545]

Gupta IR, Ryan AK. Claudins: unlocking the code to tight junction function during embryogenesis and in disease. Clin Genet. 2010; 77:314–325. [PubMed: 20447145]

Haigo SL, Hildebrand JD, Harland RM, Wallingford JB. Shroom induces apical constriction and is required for hingepoint formation during neural tube closure. Curr Biol. 2003; 13:2125–2137. [PubMed: 14680628]

Halbleib JM, Nelson WJ. Cadherins in development: cell adhesion, sorting, and tissue morphogenesis. Genes Dev. 2006; 20:3199–3214. [PubMed: 17158740]

Harris TJ, Tepass U. Adherens junctions: from molecules to morphogenesis. Nat Rev Mol Cell Biol. 2010; 11:502–514. [PubMed: 20571587]

Hildebrand JD. Shroom regulates epithelial cell shape via the apical positioning of an actomyosin network. J Cell Sci. 2005; 118:5191–5203. [PubMed: 16249236]

Hildebrand JD, Soriano P. Shroom, a PDZ domain-containing actin-binding protein, is required for neural tube morphogenesis in mice. Cell. 1999; 99:485–497. [PubMed: 10589677]

Hinck L, Nathke IS, Papkoff J, Nelson WJ. Dynamics of cadherin/catenin complex formation: novel protein interactions and pathways of complex assembly. J Cell Biol. 1994; 125:1327–1340. [PubMed: 8207061]

Hurd TW, Fan S, Liu CJ, Kweon HK, Hakansson K, Margolis B. Phosphorylation-dependent binding of 14-3-3 to the polarity protein Par3 regulates cell polarity in mammalian epithelia. Curr Biol. 2003; 13:2082–2090. [PubMed: 14653998]

Ishiuchi T, Takeichi M. Willin and Par3 cooperatively regulate epithelial apical constriction through aPKC-mediated ROCK phosphorylation. Nat Cell Biol. 2011; 13:860–866. [PubMed: 21685893]

Itoh M, Furuse M, Morita K, Kubota K, Saitou M, Tsukita S. Direct binding of three tight junction-associated MAGUKs, ZO-1, ZO-2, and ZO-3, with the COOH termini of claudins. J Cell Biol. 1999; 147:1351–1363. [PubMed: 10601346]

Ivanov AI, Bachar M, Babbin BA, Adelstein RS, Nusrat A, Parkos CA. A unique role for nonmuscle myosin heavy chain IIA in regulation of epithelial apical junctions. PLoS One. 2007; 2:e658. [PubMed: 17668046]

Ivanov AI, Hunt D, Utech M, Nusrat A, Parkos CA. Differential roles for actin polymerization and a myosin II motor in assembly of the epithelial apical junctional complex. Mol Biol Cell. 2005; 16:2636–2650. [PubMed: 15800060]

Ivanov AI, McCall IC, Parkos CA, Nusrat A. Role for actin filament turnover and a myosin II motor in cytoskeleton-driven disassembly of the epithelial apical junctional complex. Mol Biol Cell. 2004; 15:2639–2651. [PubMed: 15047870]

Jones N, Blasutig IM, Eremina V, Ruston JM, Bladt F, Li H, Huang H, Larose L, Li SS, Takano T, Quaggin SE, Pawson T. Nck adaptor proteins link nephrin to the actin cytoskeleton of kidney podocytes. Nature. 2006; 440:818–823. [PubMed: 16525419]

Kishikawa M, Suzuki A, Ohno S. aPKC enables development of zonula adherens by antagonizing centripetal contraction of the circumferential actomyosin cables. J Cell Sci. 2008; 121:2481–2492. [PubMed: 18628308]

Kojima S, Vignjevic D, Borisy GG. Improved silencing vector co-expressing GFP and small hairpin RNA. Biotechniques. 2004; 36:74–79. [PubMed: 14740488]

Kollmar R, Nakamura SK, Kappler JA, Hudspeth AJ. Expression and phylogeny of claudins in vertebrate primordia. Proc Natl Acad Sci U S A. 2001; 98:10196–10201. [PubMed: 11517306]

Koppen M, Simske JS, Sims PA, Firestein BL, Hall DH, Radice AD, Rongo C, Hardin JD. Cooperative regulation of AJM-1 controls junctional integrity in Caenorhabditis elegans epithelia. Nat Cell Biol. 2001; 3:983–991. [PubMed: 11715019]

Labouesse M. Epithelial junctions and attachments. WormBook. 2006:1–21.

Li H, Lemay S, Aoudjit L, Kawachi H, Takano T. SRC-family kinase Fyn phosphorylates the cytoplasmic domain of nephrin and modulates its interaction with podocin. J Am Soc Nephrol. 2004; 15:3006–3015. [PubMed: 15579503]

Lockwood C, Zaidel-Bar R, Hardin J. The C. elegans zonula occludens ortholog cooperates with the cadherin complex to recruit actin during morphogenesis. Curr Biol. 2008; 18:1333–1337. [PubMed: 18718757]

Lu Z, Kim do H, Fan J, Lu Q, Verbanac K, Ding L, Renegar R, Chen YH. A non-tight junction function of claudin-7-Interaction with integrin signaling in suppressing lung cancer cell proliferation and detachment. Mol Cancer. 2015; 14:120. [PubMed: 26081244]

Lynch AM, Hardin J. The assembly and maintenance of epithelial junctions in C. elegans. Front Biosci. 2009; 14:1414–1432.

Muller SL, Portwich M, Schmidt A, Utepbergenov DI, Huber O, Blasig IE, Krause G. The tight junction protein occludin and the adherens junction protein alpha-catenin share a common interaction mechanism with ZO-1. J Biol Chem. 2005; 280:3747–3756. [PubMed: 15548514]

Ozawa M, Baribault H, Kemler R. The cytoplasmic domain of the cell adhesion molecule uvomorulin associates with three independent proteins structurally related in different species. EMBO J. 1989; 8:1711–1717. [PubMed: 2788574]

Pettitt J, Cox EA, Broadbent ID, Flett A, Hardin J. The Caenorhabditis elegans p120 catenin homologue, JAC-1, modulates cadherin-catenin function during epidermal morphogenesis. J Cell Biol. 2003; 162:15–22. [PubMed: 12847081]

Raich WB, Agbunag C, Hardin J. Rapid epithelial-sheet sealing in the Caenorhabditis elegans embryo requires cadherin-dependent filopodial priming. Curr Biol. 1999; 9:1139–1146. [PubMed: 10531027]

Simon DB, Lu Y, Choate KA, Velazquez H, Al-Sabban E, Praga M, Casari G, Bettinelli A, Colussi G, Rodriguez-Soriano J, McCredie D, Milford D, Sanjad S, Lifton RP. Paracellin-1, a renal tight junction protein required for paracellular Mg2+ resorption. Science. 1999; 285:103–106. [PubMed: 10390358]

Simske JS. Claudins reign: The claudin/EMP/PMP22/γ channel protein family in C. elegans. Tissue Barriers. 2013; 1:e25502. [PubMed: 24665403]

Simske JS, Hardin J. Claudin family proteins in Caenorhabditis elegans. Methods Mol Biol. 2011; 762:147–169. [PubMed: 21717355]

Simske JS, Koppen M, Sims P, Hodgkin J, Yonkof A, Hardin J. The cell junction protein VAB-9 regulates adhesion and epidermal morphology in C. elegans. Nat Cell Biol. 2003; 5:619–625. [PubMed: 12819787]

Suzuki A, Ishiyama C, Hashiba K, Shimizu M, Ebnet K, Ohno S. aPKC kinase activity is required for the asymmetric differentiation of the premature junctional complex during epithelial cell polarization. J Cell Sci. 2002; 115:3565–3573. [PubMed: 12186943]

Umeda K, Ikenouchi J, Katahira-Tayama S, Furuse K, Sasaki H, Nakayama M, Matsui T, Tsukita S, Furuse M, Tsukita S. ZO-1 and ZO-2 independently determine where claudins are polymerized in tight-junction strand formation. Cell. 2006; 126:741–754. [PubMed: 16923393]

Vaezi A, Bauer C, Vasioukhin V, Fuchs E. Actin cable dynamics and Rho/Rock orchestrate a polarized cytoskeletal architecture in the early steps of assembling a stratified epithelium. Dev Cell. 2002; 3:367–381. [PubMed: 12361600]

Van Itallie CM, Anderson JM. The molecular physiology of tight junction pores. Physiology (Bethesda). 2004; 19:331–338. [PubMed: 15546850]

Van Itallie CM, Fanning AS, Bridges A, Anderson JM. ZO-1 stabilizes the tight junction solute barrier through coupling to the perijunctional cytoskeleton. Mol Biol Cell. 2009; 20:3930–3940. [PubMed: 19605556]

Vasioukhin V, Bauer C, Yin M, Fuchs E. Directed actin polymerization is the driving force for epithelial cell-cell adhesion. Cell. 2000; 100:209–219. [PubMed: 10660044]

Verma R, Wharram B, Kovari I, Kunkel R, Nihalani D, Wary KK, Wiggins RC, Killen P, Holzman LB. Fyn binds to and phosphorylates the kidney slit diaphragm component Nephrin. J Biol Chem. 2003; 278:20716–20723. [PubMed: 12668668]

Wang S, Cha SW, Zorn AM, Wylie C. Par6b regulates the dynamics of apicobasal polarity during development of the stratified Xenopus epidermis. PLoS One. 2013; 8:e76854. [PubMed: 24204686]

Yonemura S, Itoh M, Nagafuchi A, Tsukita S. Cell-to-cell adherens junction formation and actin filament organization: similarities and differences between non-polarized fibroblasts and polarized epithelial cells. J Cell Sci. 1995; 108(Pt 1):127–142. [PubMed: 7738090]

Zhang J, Betson M, Erasmus J, Zeikos K, Bailly M, Cramer LP, Braga VM. Actin at cell-cell junctions is composed of two dynamic and functional populations. J Cell Sci. 2005; 118:5549–5562. [PubMed: 16291727]

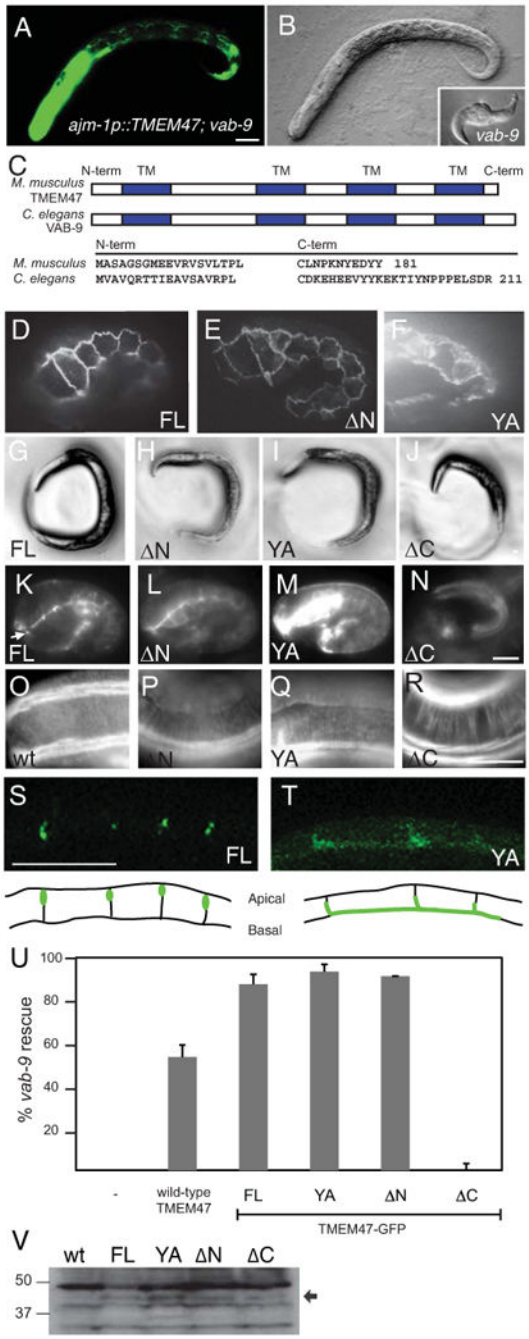

Figure 1. Murine TMEM47 functionally rescues the *C. elegans vab-9* mutation

TMEM47-GFP was expressed under control of the *ajm-1* promoter in *vab-9* mutant animals. (A) Cell junction localization of TMEM47-GFP in epidermis and expression in the pharynx. (B) Matching DIC image of panel A showing *vab-9* body and tail shape defect rescue (inset: control second larval stage *vab-9* mutant). (C) Schematic of murine TMEM47 and *C. elegans* VAB-9. TM indicates transmembrane spanning domains. The Amino terminus (N-term) and Carboxy terminus (C-term) are predicted to be intracellular. Below are shown the predicted cytoplasmic N-term and C-term amino acids. TMEM47 and VAB-9 contain 181

and 211 residues, respectively. TMEM47 canine and murine cytoplasmic domains are identical. (D-V) TMEM47 rescues *vab-9* defects. Expression of TMEM47-GFP variants in embryonic seam cells (D-F) and pharyngeal (K-N) epithelia. Full length ("FL") TMEM47-GFP and amino terminal deletion "ΔN" (E) localize strongly, but Y180/181A "YA" (F) is mis-localized basolaterally in seam cells. (G-J). Phenotypes of the variants in *vab-9(ju6)* null mutants is shown. All constructs except the C-terminal deletion "ΔC" rescue all *vab-9* phenotypes (tail, body shape, and egg-laying defects), scored as adults. (K-N) Expression of variants in the pharynx during embryonic elongation "FL" localizes normally, while "ΔN" and "YA" are not exclusively concentrated at junctions. TMEM47-GFP carboxy terminal "ΔC" was completely mislocalized from pharyngeal cell junctions (N). (O-R) Expression of Full length "FL" "N-term" and "YA" but not "ΔC" TMEM47-GFP variants restores the regular circumferential F-actin filaments in *vab-9* mutant epidermis. Anterior is to the left and the strong white band(s) indicate F-actin in muscle quadrants that run anterior to posterior just below and attached to the epidermis. The bands orthogonal to the muscle actomyosin are regularly spaced in rescued animals and are discontinuous in "ΔC" epidermis. (S, T) Lateral projections of TMEM47 FL and YA expression in dorsal epidermal cells; drawings shown below represent the TMEM47 localization observed in panels S and T, respectively. (U) Quantification of *vab-9* phenotypic rescue by untagged ("wt") TMEM47, TMEM47-GFP (FL), and TMEM47-GFP variants YA, ΔN, and ΔC. Animals were scored as adults and were only scored as rescued if all *vab-9* phenotypes were absent and animals were indistinguishable from wild type. (V) Western blot of extracts from TMEM47-GFP and variant containing strains probed with anti-GFP antibodies. Arrow indicates TMEM47-GFP fusion proteins. Scale, 10um.

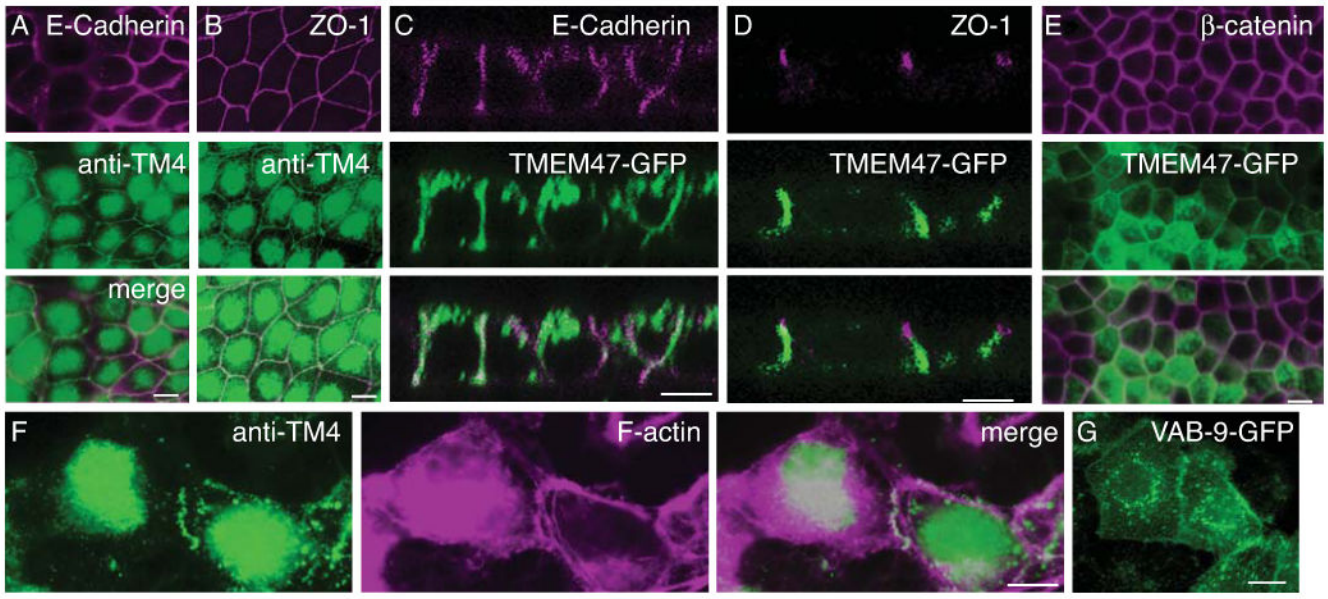

Figure 2. TMEM47 associates with adherens junctions in MDCK cells

(A,B) Immunolocalization of endogenous TMEM47 (“anti-TM4”) with E-Cadherin and ZO-1 in the apical domain of MDCK cells. The merged top focal planes (3μm) are shown. (C, D) Lateral views (Z axis) showing localization of E-Cadherin and ZO-1, respectively, relative to TMEM47-GFP. (E) Co-localization of β-Catenin with TMEM47-GFP. (F) Co-localization of endogenous TMEM47 (“anti-TM4”) with F-actin at new cell contacts in MCK cells. (G) Expression of *C. elegans* VAB9-GFP in MDCK cells shows a pattern similar to TMEM47. Gamma adjustments were made to merged images.

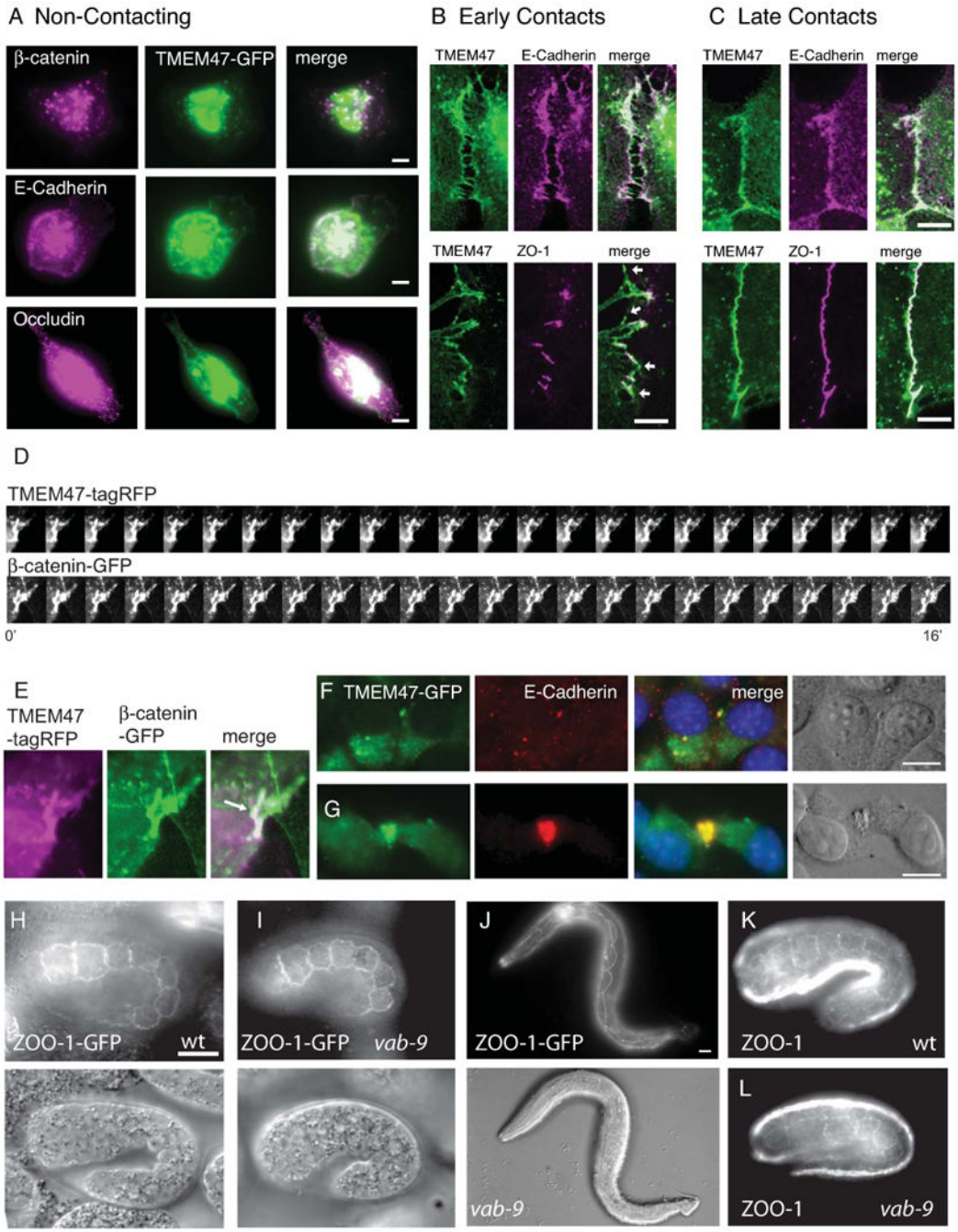

Figure 3. TMEM47 expression during junctional maturation and dependence on E-Cadherin

(A) Co-localization of TMEM47-GFP with β-Catenin, E-Cadherin, and Occludin in isolated, non-contacting MDCK cells. TMEM47-GFP is observed in cytoplasmic structures and at membranes, co-localizing with β-Catenin and E-Cadherin. Less overlap is observed with Occludin. (B, C) Co-localization of E-Cadherin and ZO-1 with TMEM47 in (B) new cell contacts (<1 hour after plating) or (C) more established cell contacts (>4 hours after plating). Arrows indicate ZO-1-free cell contacts containing TMEM47-GFP. (D) Kymograph of video recording showing similar movement of TMEM47-tagRFP (top) and β-catenin-GFP

(bottom). Total run time is 16 minutes with 24 of 58 total frames shown (E) Images of first frame from video, indicating region shown in (D). The merged image of the two tagged proteins demonstrates co-localization in a remodeling cell-cell contact. Arrows indicate the point of cell-cell contact. . (F) In L cells, which lack E-Cadherin, there was no placement of TMEM47-GFP at cell-cell contacts. (G) In L cells transfected with E-Cadherin, TMEM47-GFP now was present at cell-cell contacts and co-localized with E-Cadherin. (H-L) ZOO-1-GFP (H-J) and ZOO-1 (K,L) localize the same in wild type animals (H and K) and *vab-9(ju6)* mutants (I and J, L). Nomarski images in Columns H, I, and J match the fluorescent images above. ZOO-1-GFP localizes normally prior to development of Vab phenotypes (I) and after phenotypes are visible (fourth larval stage) (J). Scale=10um. Gamma adjustments were made to images in A, F, and G.

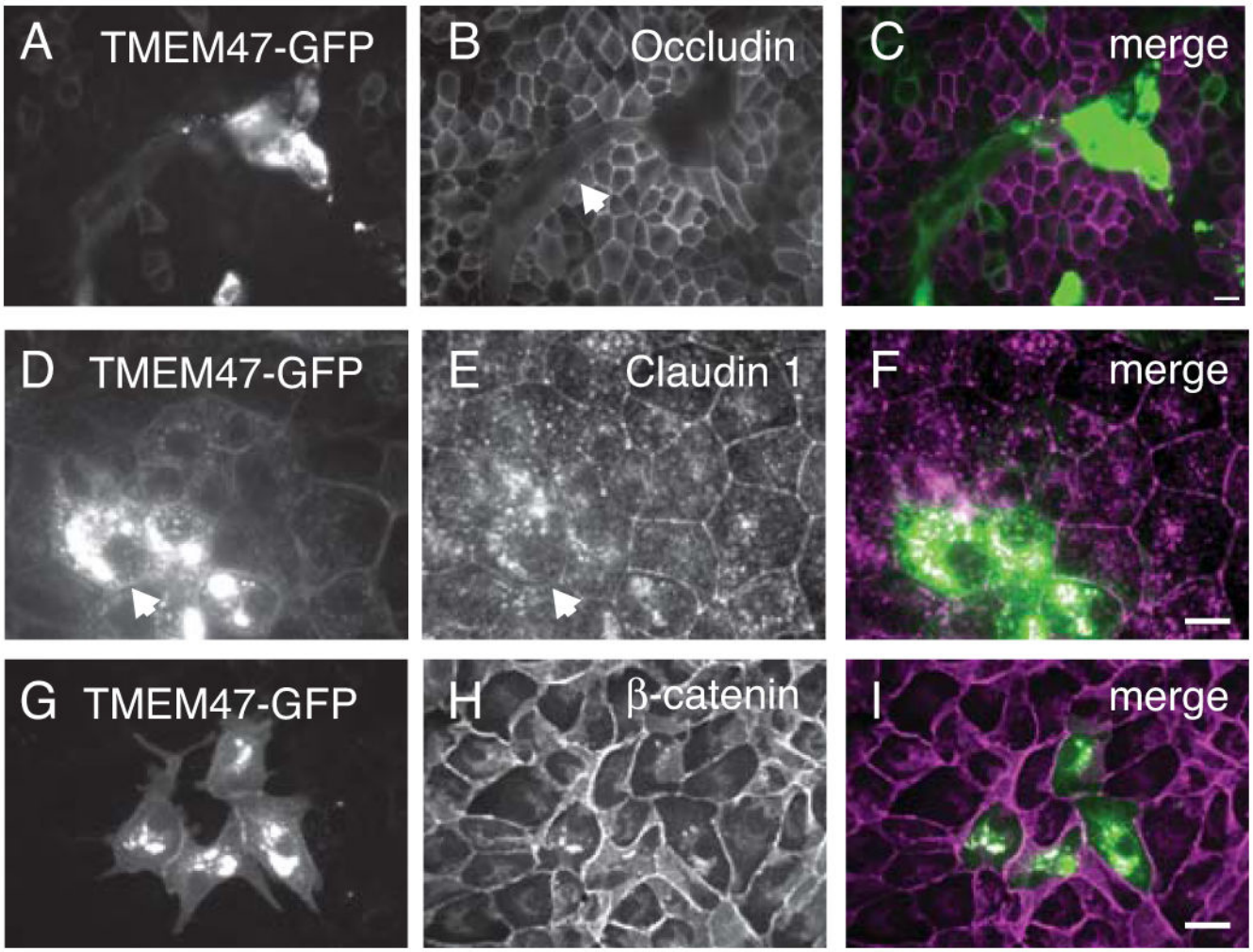

Figure 4. TMEM47 over-expression affects tight junction protein localization and F-actin organization, but not adherens junction protein localization

TMEM47-GFP over-expression in confluent MDCK cells (A,D,G) and immunolocalization of Occludin (B), Claudin 1 (E), and β-Catenin (H). Regions of TMEM47-GFP over-expression correlated with mislocalization of Occludin (B,C) and Claudin 1 (E,F), but not β-Catenin (H,I). Loss of cell membrane staining in TMEM47-GFP positive cells indicated with arrows. Scale=10um. Gamma adjustments were made to merged images (C,F,I).

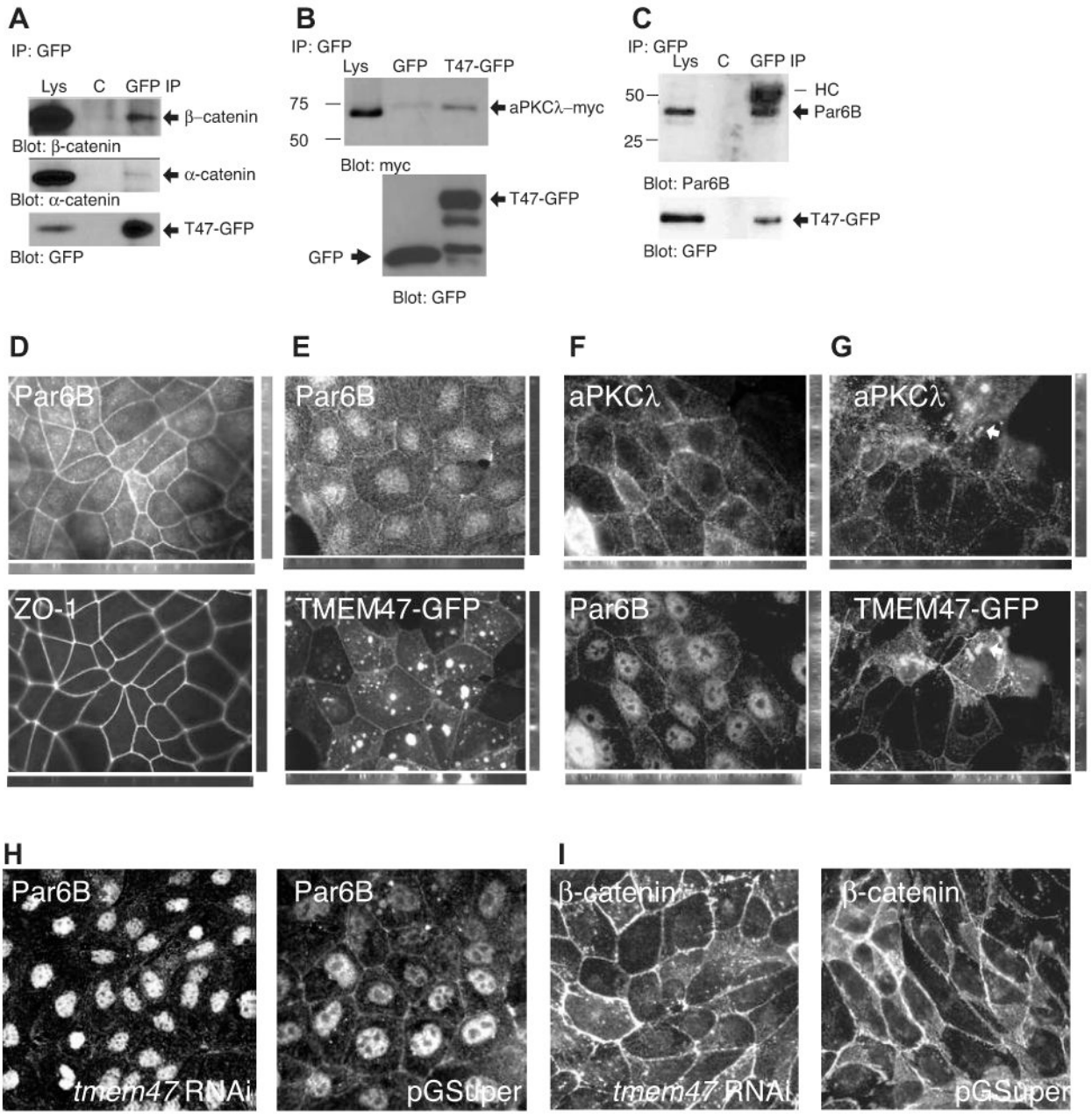

Figure 5. Association of TMEM47 with catenins and tight junction proteins Par6B and aPKCλ

(A-C) endogenous α-catenin and β-catenin (A), myc-tagged aPKCλ (B), and endogenous Par6B (C) co-immunoprecipitate with TMEM47-GFP. (D-G) Over-expression of TMEM47-GFP disrupts localization of Par6B and aPKCλ at cell junctions. (D) Normal Par6B localization in top 3um of the cell (top) compared to ZO-1 control (bottom). (E) Similar focal planes as (D) showing Par6B displaced from membrane (top) in TMEM-47-GFP expressing cells. TMEM47-GFP expression is shown (bottom). (F) aPKCλ and Par6B localization in MDCK cells. (G) mislocalized aPKCλ (top) in TMEM47-GFP over-expressing cells (bottom). Arrows indicate similar cytoplasmic aPKCλ and TMEM47-GFP localization. Thin panels show projected lateral (Z-axis) views. (H,I) *TMEM47* shRNA in

MDCK cells stained with Par6B and β-catenin, respectively. *TMEM47* RNAi is shown on the left panel and scrambled oligo in pGSuper is on the right lys = lysate, T47-GFP = TMEM47-GFP, HC = heavy chain.

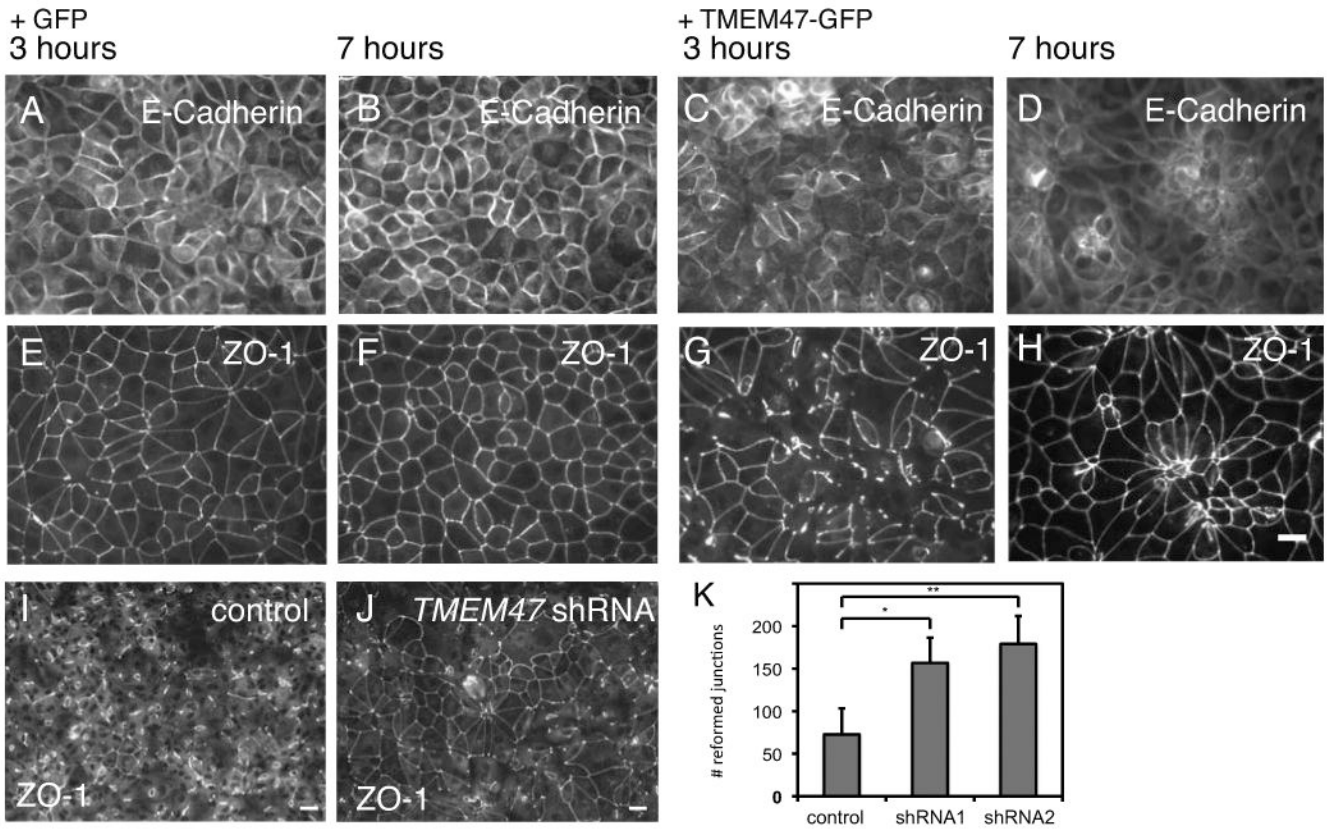

Figure 6. TMEM47 regulates cell junction reassembly following calcium switch

Confluent monolayers of MDCK cells were placed in low calcium medium to disrupt existing cell-cell junctions and then returned to normal calcium media to allow reassembly of cell junctions. (A-D) E-Cadherin expression pattern at 3 and 7 hours following low calcium incubation. Compared to normal MDCK cells (A, B), re-assembly of E-Cadherin-containing junctions were delayed in TMEM47-GFP over-expressing cells 3 hours following calcium switch (C); however junctions were re-established after 7 hours (D) but with obvious morphological defects. (E-H) Similar delays and morphological defects in ZO-1 junctional reassembly were observed in TMEM47-GFP cells (G,H) compared to control cells (E,F). (I-K) Reducing TMEM47 expression accelerates cell junction reassembly. MDCK cells transfected with scrambed oligo shRNA control vectors (I) or cells transfected with TMEM47 shRNA (J) were subjected to calcium switch and stained for ZO-1 1 hour after re-addition of calcium. TMEM47 shRNA expressing cells displayed more rapid junctional reformation after 1 hour compared to controls, quantified in (K). *P<0.027 and **P<0.015. Scale=10um.

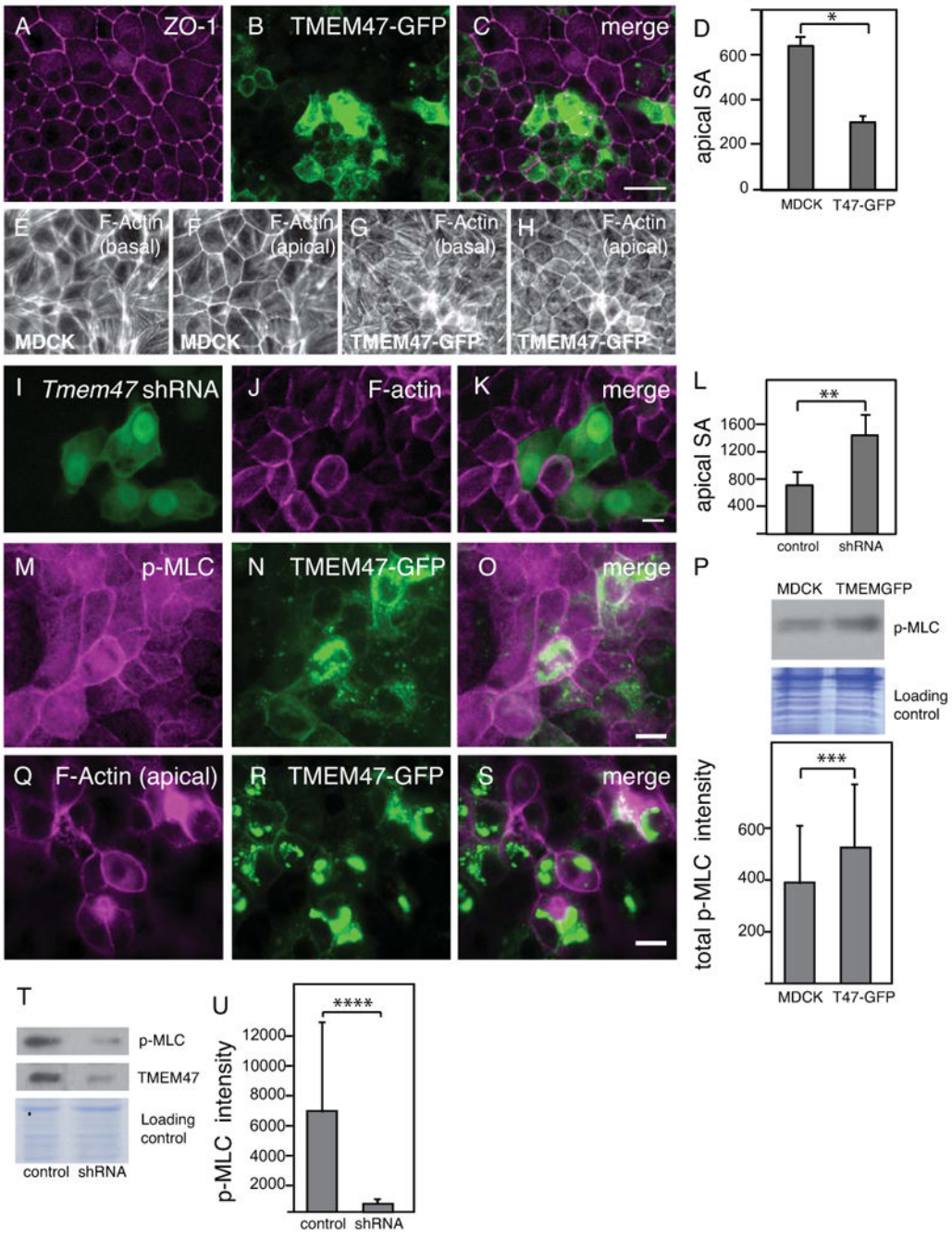

Figure 7. TMEM47 regulates apical surface area and p-MLC

(A-C) MDCK cells and MDCK cells stably expressing TMEM47-GFP were mixed and grown in confluent monolayers. (A) ZO-1 staining delineating the apical surface area. (B) TMEM47-GFP cells expressing cells (C) merged image. (D) Quantification of apical surface areas. *P<0.0001. (E-H) MDCK control cells (E,F) and TMEM47-GFP cells (G,H) phalloidin stained for F-actin reveal ventral stress fibers (E,G), and cell borders (F,H). The number of F-actin bundles/cell were not statistically different, but cell area for TMEM47-GFP was half that of MDCK cells (see text). (I-L) TMEM47 shRNA knock down cells were

immunostained for F-actin to reveal cell borders and apical surface area of expressing and non-expressing cells were measured; note that F-actin appeared reduced in shRNA cells. (L) Quantification of the apical surface area of control shRNA and TMEM47 shRNA cells. **P<0.0001. (M-O) Phosphorylated myosin light chain (p-MLC) expression (M) was increased at cell borders in TMEM47-GFP cells (N); merged in (O). (P) Despite increased concentration of p-MLC at cell junctions in TMEM47-GFP overexpressing cells, overall p-MLC levels in TMEM47 cells were not significantly greater than in MDCK cells. A representative blot of three experiments is shown in the upper panel and quantified in the third panel (*** P=0.45). (Q-S) TMEM47-GFP cells also displayed increased apical F-actin accumulation (T,U) p-MLC is reduced in *Tmem47* shRNA cells. A Representative blot (T, upper panel) of three averaged experiments (U) is shown. **** P= 0.0372. (T, second panel) Knockdown efficiency of *TMEM47* culture was determined by Western blotting. SA = Surface Area. Scale=10um., Gamma adjustments were made to merged images C,K, and O.